Strain-induced disorder, phase transformations, and transformation-induced plasticity in hexagonal boron nitride under compression and shear in a rotational diamond anvil cell: *In situ* x-ray diffraction study and modeling

Valery I. Levitas,[a] Yanzhang Ma, and Javad Hashemi
Department of Mechanical Engineering, Texas Tech University, Lubbock, Texas 79409-1021 and Center for Mechanochemistry and Synthesis of New Materials, Texas Tech University, Lubbock, Texas 79409-1021

Mark Holtz
Department of Physics, Texas Tech University, Lubbock, Texas 79409-1021

Necip Guven
Department of Geosciences, Texas Tech University, Lubbock, Texas 79409-1021 and Center for Mechanochemistry and Synthesis of New Materials, Texas Tech University, Lubbock, Texas 79409-1021

(Received 17 January 2006; accepted 2 May 2006; published online 25 July 2006)

Plastic shear significantly reduces the phase transformation (PT) pressure when compared to hydrostatic conditions. Here, a paradoxical result was obtained: PT of graphitelike hexagonal boron nitride (hBN) to superhard wurtzitic boron nitride under pressure and shear started at about the same pressure (~10 GPa) as under hydrostatic conditions. In situ x-ray diffraction measurement and modeling of the turbostratic stacking fault concentration (degree of disorder) and PT in hBN were performed. Under hydrostatic pressure, changes in the disorder were negligible. Under a complex compression and shear loading program, a strain-induced disorder was observed and quantitatively characterized. It is found that the strain-induced disorder suppresses PT which compensates the promotion effect of plastic shear. The existence of transformation-induced plasticity (TRIP) was also proved during strain-induced PT. The degree of disorder is proposed to be used as a physical measure of plastic straining. This allows us to quantitatively separate the conventional plasticity and transformation-induced plasticity. Surprisingly, it is found that TRIP exceeds the conventional plasticity by a factor of 20. The cascade structural changes were revealed, defined as the reoccurrence of interacting processes including PTs, disordering, conventional plasticity, and TRIP. In comparison with hydrostatic loading, for the same degree of disorder, plastic shear indeed reduces the PT pressure (by a factor of 3–4) while causing a complete irreversible PT. The analytical results based on coupled strain-controlled kinetic equations for disorder and PT confirm our conclusions.
 [DOI: 10.1063/1.2208353]

I. INTRODUCTION

A. Effect of plastic shear on phase transformations

It is well known that the superposition of large plastic shear on high pressure drastically changes the microstructure, mechanism, thermodynamics, and kinetics of phase transformation (PT).[1–4] In particular, the plastic shear produced due to superposition of rotation in a rotational diamond anvil cell (i) significantly reduces the PT pressure (by a factor of 2–5), (ii) promotes the formation of novel phases that would not appear without shear, (iii) substitutes reversible PTs with irreversible phase transformations, and (iv) leads to strain-controlled kinetics. However, despite the strong fundamental and applied interest, quantitative characterization and understanding of the above phenomena are lacking. In this paper, we will raise the issue that some basic differences between the plastic *strain-induced PTs* under high pressure and *pressure-induced PTs* have not been recognized by high pressure community. Both pressure-induced (under hydrostatic conditions) and stress-induced (under nonhydrostatic conditions) phase transformation initiate predominantly at preexisting defects when the external stresses do not exceed the macroscopic yield strength.[5] On the contrary, strain-induced phase transformation occurs by nucleation at new defects (stress concentrators) generated during plastic flow without a growth stage.[5] Time is not a relevant parameter for strain-induced phase transformation; instead, strain-controlled kinetics is considered. Thus, strain-induced transformations require a completely different thermodynamic and kinetic description as well as experimental characterizations. An understanding of the reasons and physical mechanisms of the effect of plastic shear on phase transformations is extremely important from the point of view of basic physics, searching for new materials and improvement of high pressure technologies for material synthesis. In the following paragraphs, we will highlight some of the chal-

[a]Electronic mail: valery.levitas@ttu.edu

lenges associated with understanding strain-induced PTs under high pressure.

B. Effect of turbostratic stacking faults

Turbostratic stacking faults (TSFs) are formed in hexagonal or rhombohedral crystals by relative rotation or displacement of two parts of a lattice in (001) planes to arbitrary positions causing disorder.[6–8] The degree of this three-dimensional disorder is characterized by the concentration of TSF, s. Generally, phase transformation pressure increases with increasing disorder and kinetics is suppressed. In particular, in shock experiments, at a pressure of 20 GPa, volume fraction of wurtzitic boron nitride (wBN) intensively grows from 0 (for high level of disorder, $s=0.1$) to 0.8 (for a significantly lower level of disorder, $s=0.03$). wBN was not observed for $s>0.1$. Although the above results show the importance of s in formation of wBN, very little is known about its influence during the phase transformation process; in the literature only few publications report measurement of s before the transformation process.[6–8] To truly characterize phase transformation in BN and other hexagonal and rhombohedral structures, one must locally measure the evolution of disorder s before and during the phase transformation process. The knowledge of the evolution of disorder s can be used for the reduction of transformation pressure and optimization of the process.

C. Homogeneity of pressure distribution

Usually, the plastic compression of samples in a diamond anvil cell causes a large pressure gradient, which complicates the characterization of PTs.[3,4] The pressure sharply grows during PT if a stronger phase appears and vice versa.[3,4,9,10] For example, for B1 to B2 phase transformation in KCl, pressure in the center was 2.7 GPa before rotation and reached 5.5 GPa after rotation by 10° (while PT could be completed at 2.7 GPa).[4] This pressure increase at a fixed force serves as a positive mechanochemical feedback and further promotes PT, leading to complete PT during small rotation. Clearly this sudden jump in pressure due to plastic shear does not allow any *in situ* and timely experimental analysis of the kinetics. Because of (a) radial flow of material particles, (b) strong pressure variation in the transformed region during the phase transformation, (c) completion of PT during small rotation, and (d) inaccuracy of pressure measurement in the region with high pressure gradient, quantitative characterization of strain-induced PTs is practically impossible and has never been attempted. Moreover, if the product phase is much stronger than the parent phase, PT leads to a very high pressure in the transformed phase, causing the fracture of the anvil. This was observed in (Ref. 10) for rhombohedral boron nitride (BN) to cubic boron nitride (cBN) PT, where the pressure grew from 5.6 GPa to an estimated pressure range of 60–76 GPa at the center. Consequently, one of the basic problems in the study and characterization of strain-induced PTs is *to create a homogeneous stress state in the transformed region*, which does not vary significantly during the PT. This is important not only for research but also from the perspective of the development of technology for strain-induced material syntheses. Achieving a homogeneous pressure growth is quite an ambitious task for hexagonal boron nitride (hBN)→wBN PT due to extremely large volume reduction by a factor of 1.53.

D. Phase transformation in BN system

Phase transformation of hBN and rBN into dense superhard modifications such as wBN and cBN is of great fundamental and applied importance. Wurtzitic boron nitride and especially cBN have wide technological applications due to their hardness (second only to diamond) and their superior chemical and thermal stabilities. In industry, the superhard phase, cBN, is generally synthesized through pressure-induced PT under pressures greater than 4 GPa, temperatures exceeding 1600 K, and using metal alloys as catalyst. wBN is synthesized by explosive loading. Strain-induced synthesis of cBN and wBN under quasistatic loading, room temperature, and without catalyst could be of great fundamental and technological importance. The martensitic PT of hBN to wBN represents a *unique case of PT with extremely large volume reduction* (by a factor of 1.53). Usually martensitic PT is shear dominated but in BN volumetric transformation strain prevails. Large volumetric transformation strain ε_0, during any PT, creates large internal stresses which in combination with external shear stresses lead to strong transformation-induced plasticity (TRIP).[8,11,12] However, TRIP (to our knowledge) has never been experimentally confirmed in high pressure experiments in diamond anvil cell. The main reason is that usually TRIP is measured experimentally for stress-induced phase transformation when conventional plasticity is absent. For strain-induced PT, it is difficult to separate the conventional plasticity and TRIP.

E. Objectives

We are not aware of any study of BN in rotational diamond anvils, as well as of *in situ* synchrotron x-ray diffraction research of any material in rotational diamond anvils. *In situ* evolution of disorder has not been studied under high pressure. The objectives of this work were (a) to find theoretically and produce experimentally the conditions for homogeneous pressure distribution and growth under compression and rotation before and during phase transformation; (b) to perform an *in situ* study of the strain-induced disordering and phase transformation in hBN up to 25 GPa in rotational diamond anvil cell, as well as pressure-induced disordering under hydrostatic conditions, using synchrotron x-ray diffraction; (c) to justify s as a physical measure of plastic straining, use it to prove the existence of transformation-induced plasticity, and to quantify TRIP; and (d) to develop and study a model describing the interaction between conventional plasticity, disorder, PT, and TRIP.

Experimental methods are described in Sec. II. Conditions for quasihomogeneous pressure distribution were derived in Sec. III and confirmed experimentally in Sec. IV. The main experimental results are also reported in Sec. IV. In particular, a paradoxical result was obtained: The phase transformation of hBN to wBN under pressure and shear started at 9.6 GPa and under hydrostatic conditions at

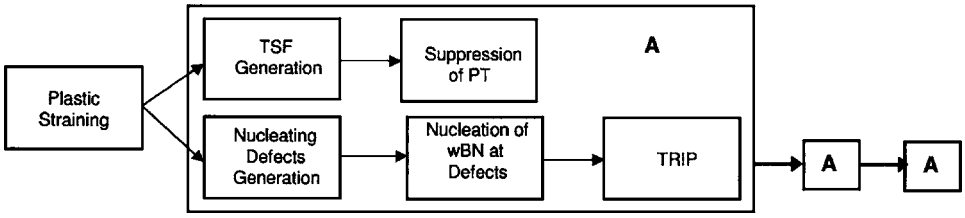

FIG. 1. The cascading mechanism of structural changes during continuous rotation of an anvil. Plastic straining generates both turbostratic stacking faults, which suppress the phase transformation, and nucleating defects (e.g., dislocation pileups and various tilt boundaries), which promote the phase transformation. Phase transformation under shear stresses produces strong transformation-induced plasticity; TRIP, in the same way as conventional plasticity, generates the turbostratic stacking fault (the dominating part) and new nucleating defects; the new nucleating defects again promote the phase transformation, which produces transformation-induced plasticity; and so on. When rotation stops, each of these processes stop as well.

10.4 GPa, which are very similar. This paradox was resolved by identifying the strain-induced disorder that suppresses PT and compensates the promotion effect of plastic shear. Section V is devoted to the modeling and analyses of the results. The cascade structural changes were revealed (Fig. 1): Plastic straining generates TSFs (which suppress the PT) and nucleating defects (which promote the PT). PT under shear stress produces strong TRIP; TRIP, similar to conventional plasticity, generates disorder (the dominating part) and new nucleating defects; the new nucleating defects again promote the PT, which produces TRIP; and the process repeats itself. Concluding remarks are made in Sec. VI.

II. EXPERIMENTAL METHODS AND DATA PROCESSING

High purity grade hBN with an average crystallite size of 4 μm and oxygen (major impurity) concentration of 0.4% was analyzed under pressure and shear. The BN powder had a random initial orientation without any initial texture. For each sample, a stainless steel gasket (T301) with the corresponding geometric parameters reported below was used without pressure transmitting media. Experiments were performed using a rotational diamond anvil cell (see Fig. 2) with a culet radius of 250 μm (for the first and second samples) and 145 μm (for the third sample). A detailed description of a similar rotational diamond anvil cell and the corresponding measurement techniques can be found in Ref. 4. One experiment was performed at Texas Tech University. The x-ray analysis (P1160-50, Cu $K\alpha$ radiation) of this specimen and two other *in situ* experiments were conducted at Brookhaven National Laboratory. Sample was compressed to some pressure followed by the rotation of the anvil at a fixed axial force. The procedure of increasing force and superimposing rotation was repeated multiple times. To reduce potential strain-induced texture, rotation of an anvil was performed in both directions. The loading history for the second sample is reflected in Table I. During a rotation increment ϕ, shown in Table I, pressure varies from the value shown in the previous loading step to the value in the current step. Synchrotron x-ray diffraction was carried out at beam lines X17C and X17B using the energy dispersive method; for details see Ref. 14. A 1% systematic error is expected in energy dispersive measurements. Different 2θ angles were chosen to eliminate fluorescence and escape lines. The beam size was confined to 16×8 μm^2. In order to compare data from the same point of the sample in the chamber, the x-ray spot was positioned at the center of the gasket hole. Pressure distribution was measured by the ruby fluorescence technique.[15] The relative locations of ruby chips (size <0.5 μm) in the gasket hole were measured in micrometers with respect to the edge of the hole. In Table I, the rows that do not have a pressure value indicate that no pressure measurements were made. The thickness of the sample under load was measured using an electric capacity sensor described in Ref. 4. The volume fractions of wBN and hBN were, respectively, estimated using experimentally determined relationships $c_1=45.009x^3+18.737x^2+34.872x$ and $c_2=57.269y^3-162.26y^2+205.72y$ (plotted in Ref. 8), where $x=I^w_{110}/(I^w_{110}+I^h_{110})$, $y=I^h_{100}/(I^w_{100}+I^h_{100})$, and I_{jkl} is the integral intensity of ijk diffraction lines of wBN (superscript w) and hBN (superscript h). Both equations produce similar results. The average wBN volume fraction c was determined by the equation $c=c_1/(c_1+c_2)=1-(c_2/(c_1+c_2))$. The concentration of TSF, s, was determined by a method developed by Kurdyumov[5–7,16] through measurement of the broadening of the width of diffraction lines. The widths of diffraction lines B_{hkl} were measured at half of the maximum value. Generally, broadening can be caused by stress fields of various defects and the main task is to separate the effect of TSF. The key idea is that turbostratic stacking faults, s, broaden the hkl diffraction lines for $l\neq 0$ and have no effect on the diffraction lines with $l=0$. Thus, some relative measure of the width of any peak affected by TSF with respect to the width of peak unaffected by TSF can be

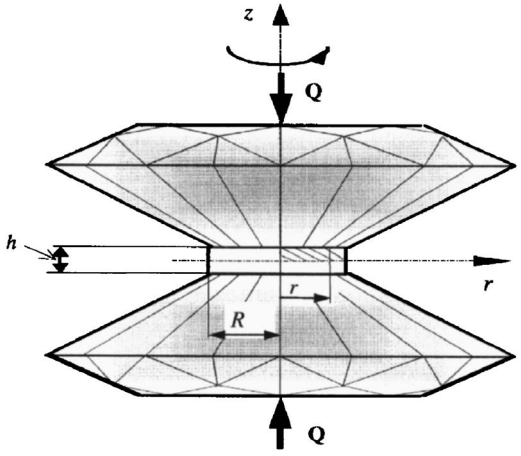

FIG. 2. A schematic of the rotational diamond anvil cell showing the critical dimensions of the cell and the gasket.

TABLE I. The loading history, disorder, and phase fraction data. During a rotation increment ϕ, pressure varies from the value shown in the previous loading step to the value in the current step. Hyphen indicates measurements at locations other than center within the same loading step. Asterisk indicates no pressure measurements were performed at that point.

	p (GPa)	ϕ (deg)	r (μm)	B_{110}	B_{112}	β°	s	l^W_{110}	l^h_{110}	x	c_1	l^w_{100}	l^h_{100}	y	c_2	c
1	0	0	0	0.43	0.61	0.29	0.077									0
2	2.1	0	0	0.43	0.62	0.33	0.085									0
3	3.8	0	0	0.45	0.67	0.36	0.095									0
—	4.2	0	40	0.46	0.67	0.34	0.091									0
4	*	20	0	0.46	0.64	0.31	0.082									0
5	3.8	50	0	0.46	0.68	0.36	0.094									0
6	6.4	0	0	0.47	0.69	0.37	0.098									0
7	*	20	0	0.43	0.67	0.39	0.103									0
8	5.8	70	0	0.44	0.75	0.49	0.127									0
—	6.6	0	30	0.48	0.72	0.40	0.106									0
9	9.6	0	0	0.5	0.74	0.40	0.107	720	4045	0.15	5	1448	19534	0.93	95	0.05
10	*	25	0	0.6	1.37	1.10	0.267	1481	271	0.84	70	10892	2074	0.15	30	0.7
—	*	0	40	0.5	1.18	0.96	0.238	402	116	0.77	60	3386	894	0.2	35	0.63
11	10.3	70	0	0.53	1.38	1.17	0.278	2623	847	0.75	58	13885	2972	0.17	32	0.64
12	10.6	205	0													1
13	13.9	0	0													
14	*	30	0													
15	25.2	30	0													

used to cancel out the effect of all defects but TSF. The physical (relative) broadening β of hkl diffraction lines caused only by TSF was defined as $\beta=B_{hkl}-B^2_{hk0}/B_{hkl}$ (in degrees).[5–7,16] The experimental relative broadening β was used together with the relationship obtained from the simplified theory: $\beta=328.8d^2_{hk0}(s/\sqrt{1-s})\tan\theta$, where d_{hk0} (in nanometers) is the interplanar spacing and θ is the Bragg angle. The structural study was performed by powder x-ray diffractometry, measurement of the broadening of (112) diffraction lines relative to the reference line (110) (i.e., $h=k=1$, $l=2$), and measurements of d_{110} and the Bragg angle. Then s was determined from the above equation. In our experiments, we are using the energy dispersive method of gathering information relative to broadening of the peaks of interest. The equations developed by Kurdymov[5–7] are based on values gathered by the angle dispersive approach. However, we assume that the application of those equations will serve as a first order approximate of the values of s. Additionally, the relative broadening value β may also be used as a measure on its own. The intensity of each reflection in energy dispersive polychromatic x-ray diffraction will be attenuated according to the energy of that reflection, whereas the attenuation will be the same for all the reflections obtained with a monochromatic Bragg-Brentano diffractometer.[17] Although the energy dispersive measurements cannot provide absolute intensity values of the diffractions, the energy effect on intensity of a selected diffraction peak can be neglected since the energy shift is limited (within 1 keV). Since determination of the volume fraction of wBN and degree of disorder s is based on the relative intensities of the peaks of the same diffraction lines, we believe that, as a first approximation, they are independent of the beam intensity. The profile of a single reflection, however, is not expected to be seriously affected by strain. In addition, two other samples were studied, *in situ*, under hydrostatic conditions using argon (which remains hydrostatic even above 10 GPa) as the pressure transmitting medium. Some preliminary results were presented in Ref. 13.

III. CONDITIONS FOR QUASIHOMOGENEOUS PRESSURE

A. Compression stage

Pressure gradient, $\partial p/\partial r$, in a sample under compression is caused by the shear stress τ_r acting in the radial direction at the interface between the diamond and the sample. This is determined according to the well-known[18] simplified equilibrium equation $\partial p/\partial r=-2\tau_r/h$, where h is the current sample thickness. For an intensive radial flow in a thin disk (without rotation), $\tau_r=\tau_y=\sigma_y/\sqrt{3}$, where τ_y and σ_y are the yield strengths in shear and compression based on von Mises yield condition. The solution of the above one-dimensional equation is in good agreement with the slip-line solution of the exact two-dimensional equations for $r\geqslant h$.[18] In the initial stages of the compression, or in the case when radial displacement of the particle is limited, shear stress can be much smaller than τ_y. A possible method to produce high homogeneous pressure is to use a gasket with a yield strength higher than that of the sample. Then the pressure in the gasket grows intensively and prohibits (limits) the radial flow in the specimen. This is the case for hBN and stainless steel gasket. As it follows from the slip-line solution for the thin solid cylinder,[18] in the central part of the cylinder, where $r/h<1$, a weakly deformed zone appears. Shear stress and pressure gradient vary from their maximum values to zero at the axis of symmetry. For a cylindrical specimen with $r_s/h<0.5$, where r_s is the sample radius, plastic deformation is concentrated along the conical slip surfaces inside the specimen and shear frictional stresses as well as the pressure gradient are approximately zero. The above is true prior to pronounced barreling. Thus, the ratio $r_s/h<0.5$ would be perfect for a

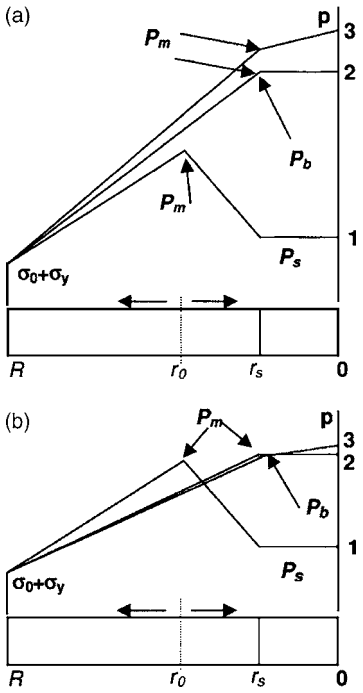

FIG. 3. Pressure distribution in the sample during (a) compression and (b) rotation under constant load. For pressure in the gasket greater than the pressure in the sample, material to the right of the neutral radius r_0 moves to the center of specimen (curve 1), causing change in the sign of frictional stress and pressure gradient. In the opposite case, plastic flow in the specimen will occur from the center and frictional stress will grow together with pressure gradient in the specimen (curve 3).

homogeneous pressure in the specimen inside the hole in the gasket. However, the disadvantage is that the specimen becomes too small with the given dimensions. We will use $r_s/h<1$ combined with minimization of the radial displacement of the cylindrical boundary of the specimen (ideally the radial displacement of the boundary between the gasket and specimen has to be zero). Integrating the equilibrium equation for a gasket with external radius R and utilizing the boundary condition $p=\sigma_0+\sigma_y$ for $r=R$, we obtain

$$p(r)=\sigma_0+\sigma_y\left[\frac{1+2(R-r)}{\sqrt{3}h}\right]. \tag{1}$$

Here σ_0 is the lateral pressure at $r=R$ due to the external support of the part of the gasket outside the working region of the anvil ($r>R$). If plastic flow occurs from the center of the sample, then Eq. (1) is valid up to r_s. The pressure at the gasket-sample boundary, $p_b=p(r_s)$, is the maximum pressure in the gasket (Fig. 3, curves 2 and 3). If for some thickness h, $p_b=p_s$, where p_s is the pressure inside the specimen, and a specimen deforms elastically, then the condition $dp_b/dt=dp_s/dt$ results in

$$\sigma_y\left(\frac{2}{\sqrt{3}}\frac{R-r_s}{h}\right)\frac{\dot{h}}{h^2}=\frac{\partial p_s}{\partial \varepsilon_e}\frac{\dot{h}}{h}, \tag{2}$$

where ε_e is the volumetric elastic strain of the tested material and for $r_s=$const one has $d\varepsilon_e/dt=\dot{h}/h$. This condition cannot be fulfilled during the whole process, because it requires a special relationship among the elastic properties of the specimen, plastic properties of gasket, and the thickness of the specimen. Between two alternatives of increasing or decreasing the radius of the specimen r_s, we chose the latter one. The first reason is that this decreases the ratio r_s/h, which in turn reduces the effect of friction. Second, while any decrease in radius r_s can be due to elastic compression only (for void-free material), an increase in radius r_s can be also due to plastic flow and may be much larger. The pressure distribution is presented schematically in Fig. 3(a) (curve 1), where r_0 is the neutral radius corresponding to the locations of zero radial velocity of material and the maximum pressure in the gasket, $p_m=p(r_0)$. The material at $r>r_0$ moves to the center of specimen, causing a change in the sign of the frictional stress and therefore pressure gradient, according to equation $\partial p/\partial r=-2\tau_r/h$. We can ensure a decrease in radius r_s if we fulfill the inequality $p_m>p_s$ during all stages of compression. If, during additional compression, pressure in the specimen grows more intensively than in the gasket, then the neutral radius moves toward the sample. As a result, less gasket material flows toward the sample and at some h, the equality $p_b=p_m=p_s$ will be reached (Fig. 3, curve 2). Under additional compression, plastic flow in the specimen will occur from the center, and shear frictional stress will grow together with pressure gradient in the sample (Fig. 3, curve 3). This illustrates the importance of inequality $p_b>p_s$ for homogeneous pressure distribution in the sample.

The geometric parameters of the gasket and specimen are determined based on the following scheme. By measuring two values of pressure $p_m=p_b$ for two different thicknesses, we estimate parameters σ_0 and σ_y assuming that they are approximately constant for both thicknesses. Note that under an accumulated plastic strain q greater than 1, the yield strength is independent of strain and strain history.[18] Let us choose the maximal pressure of interest, p_s, in the specimen and $r_s/h=1$. We can then find, from the condition $p_b=p_s$, the ratio R/h and consequently h under maximum load and $r_s=h$ (assuming that r_s does not vary during plastic flow).

We report below three experiments. In the first experiment, $R=250$ μm, $r_s=150$ μm, $p_b=10$ GPa for $h=58$ μm, and $p_b=25$ GPa for $h=11$ μm, we obtained $\sigma_0=4.73$ GPa and $\sigma_y=1.76$ GPa. Planning a maximum pressure of $p_s=10$ GPa, before phase transformation, we obtain $R/h=2.7$ and $h=r_s=92.5$ μm. In the second experiment, we choose the initial radius of 100 μm, taking into account the decrease in its radius at the initial stage of compression, in particular, due to the initial porosity of hBN. For the third sample, $R=140$ μm, $p_s=9$ GPa, and we obtain $h=r_s=64.8$ μm. In experiment, we chose $r_s=60$ μm.

B. Rotation of the anvil at constant force

In a thin solid specimen, prior to PT, rotation of the anvil leads to a change in the direction of shear frictional stress; because the magnitude of shear stress is τ_y, then the shear stress in radial direction τ_r becomes smaller. This leads to a reduction in the thickness of the specimen; however, the pressure distribution is the same before and after rotation.[4,8,19] For the precursor material (which is in an elastic state) in the gasket, the reduction of thickness due to rotation leads to an increase in pressure p_s and shift of the

neutral radius r_0 to the center of the disk [Fig. 3(b), curves 1 and 2]. Alternatively, if before rotation the precursor material flows from the center, then under rotation it will continue to flow from the center and the ratio r_s/h, the friction, and the pressure gradient will increase [Fig. 3(b), curve 3]. This is one more argument that the choice of parameters leading to the reduction of the specimen radius during the compression is favorable for the reduction of pressure gradient in the sample.

If a specimen possesses some porosity which does not disappear during compression, then the torsion of the specimen due to rotation of the anvil will lead to reduction of porosity. For powder materials, plastic shear facilitates motion of particles leading to better packing. For compact materials, the shear stress near the voids contributes to the yield condition allowing the closing of voids under smaller compression. In both cases, possible fracture, in the vicinity of the voids, due to shear stress and pressure facilitates better packing. Thus, due to plastic volumetric strain, pressure growth in the specimen during rotation will be smaller than for compact material.

A similar situation will occur in the course of PT in the specimen during rotation under constant force, when a part of the gasket moves to the center. Because of the transformation volume decrease and changes in elastic properties, pressure may slightly reduce or grow, depending on the specific parameters. The situation in which plastic flow from the center occurred before PT was considered in Ref. 8. The reduction in thickness due to rotation of the anvil compensates and even overcompensates the volume decrease due to PT. If the product phase has a yield stress higher than the parent phase, then, according to the equilibrium equation, pressure gradient and the pressure in the center of the specimen increase. This is the so-called pressure self-multiplication effect.[3,4,20,21] As it was discussed in the Introduction, this leads to significant problems in the characterization of PT and in the possible fracture of the diamond. Choosing $r_s/h<1$ after compression and the overall geometry of the gasket leading to the flow to the center will allow us to avoid essential pressure heterogeneity during the PT.

Note that under large rotation of void-free material, due to significant reduction in thickness, it is impossible to avoid the flow from the center and increase in radius of the sample. However, if before initiation of the rotation the radial shear stress was negligible, then it has to be small during the rotation because of the significant torsional component of shear stress and constant axial force. This conclusion will be confirmed experimentally. Thus, the main limitation for a sample design is $r_s/h<1$ after compression and before rotation of the anvil.

IV. EXPERIMENTAL STUDY

A. First sample

A preindented stainless steel gasket with an initial 125 μm radius hole and a thickness of 212 μm was densely packed with hBN. After compression to 5 GPa, at the sample center, the hole containing the hBN was observed to grow. At 10 GPa the thickness of the sample was 58 μm. The rotation of the anvil by 120° resulted in a reduction in thickness to approximately 24 μm without discernable additional enlargement of the hole. Pressure was then increased to 25 GPa with a measured sample thickness of 11 μm. During a subsequent rotation of the anvil in both directions for a total of 240°, the thickness of the sample reduced to 5 μm.

X-ray diffraction was measured in different spots of the unloaded sample along the radial direction with a 30 μm step and gave identical results. A 360° chi rotation was performed during the measurements at the center of the sample. The extracted pattern can be well indexed into that of wBN. We notice that the broad peak at about 0.21 nm can also be indexed into the (111) diffraction of the cBN, or to the double peaks of the (111) of cBN and (002) of wBN. However, the intensity of this peak is very low and there are no other diffraction lines of cBN to confirm its existence. The percentage of cBN, if there is any, is very low and therefore the conclusion may be made that a complete hBN→wBN phase transformation took place. The results of this test were used to determine parameters σ_0 and σ_y and the geometric parameters of the gasket to create homogeneous pressure in the sample (see Sec. III).

B. Second sample

A stainless steel gasket with a 100 μm radius hole and an initial thickness of 212 μm was packed with hBN. As with the first experiment, a very thin layer of very fine ruby powder (grain size <0.5 μm) was placed on one side of the sample to measure pressure. The laser spot was manipulated to achieve a spatial resolution of 10–20 μm for pressure measurements across the diameter. During loading, the ruby R1 and R2 lines broadened gradually but remained resolvable. The loading program, results of measurements of turbostratic stacking fault concentration s, and volume fraction c of wBN are presented in Table I.

1. Variation of pressure distribution and x-ray patterns

Figure 4 shows pressure recorded from ruby fluorescence, along the anvil diameter. The figure demonstrates that we succeeded in achieving an almost homogeneous pressure distribution at all stages of compression up to 10 GPa. Rotation of the anvil (when it did not result in PT) did not introduce inhomogeneity in the pressure distribution and did not change it appreciably. Rotation of the anvil at a pressure of 9.6 GPa leads to hBN→wBN phase transformation as seen in our x-ray diffraction data, Fig. 5. Rotation by 95° increases the pressure at the periphery of the sample by 2 GPa and does not change the pressure at the center. Pressure growth means that the volume reduction due to PT is compensated by the reduction in thickness due to rotation, and higher elastic and plastic properties of wBN cause a slight pressure growth. This indicates that PT is more intensive in the periphery of the sample (where plastic shear is maximal). An additional rotation of $\phi=205°$ completes the PT in the whole specimen, reduces the pressure at the periphery, and ends with a practically homogeneous pressure, $p=10.6$ GPa.

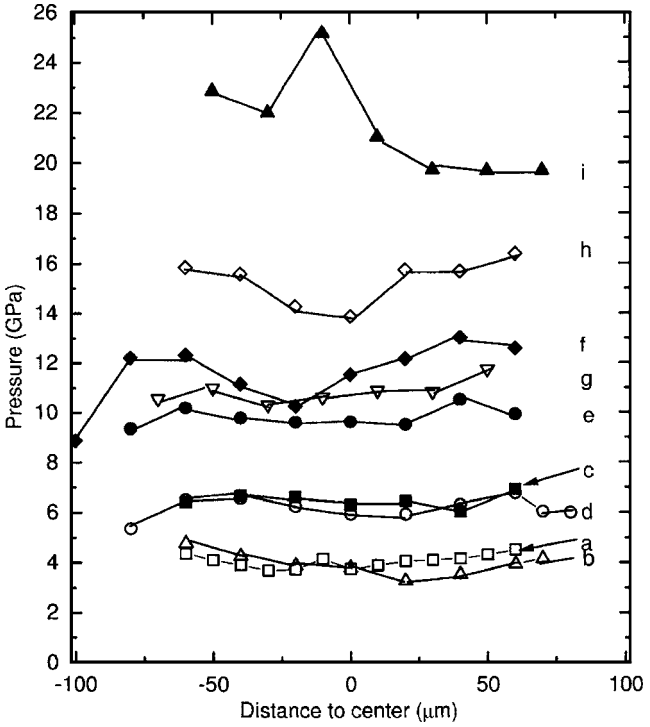

FIG. 4. Pressure distribution along the radial direction of the sample chamber. (a) Pressure increase (PI); (b) rotation, $\phi=70°$; (c) PI; (d) $\phi=90°$; (e) PI; (f) $\phi=95°$; (g). $\phi=205°$; (h) PI; and (i) $\phi=60°$. The measurement at 100 μm on curve f (8.8 GPa) is at the distorted edge of gasket.

Comparing the pressure distribution before rotation and after completing the PT [i.e., comparing lines (e) and (g) in Fig. 4], we conclude that the *homogeneous* pressure self-multiplication effect was observed for the first time. The reason for the pressure increase is the reduction in the thickness of the sample during the rotation of the anvil; the reduction in sample thickness overcompensates the volume decrease during the PT. As a result, the reduction in thickness under a fixed load leads to an increase (decrease) in pressure in the phase with the higher (lower) elastic and plastic properties. This phenomenon and its description are similar to those for heterogeneous pressure self-multiplication effect analyzed in Ref. 19. In both cases, in order to keep the same axial force before and after rotation, the pressure in the gasket decreases [see Fig. 3(b), curves 2 and 3]. In Ref. 19, the pressure in the external part of the sample decreases due to the same reason [see Figs. 2 and 10(b) in Ref. 19]. The reason for uniform pressure growth, in this case, is related to the uniform pressure state before the PT which causes almost uniform phase transformation in the sample. The advantage of the homogeneous pressure self-multiplication effect in comparison with an inhomogeneous one known in the literature[3,4,9,20,21] is that the pressure growth cannot be large. The heterogeneous pressure self-multiplication effect was observed during rotation when plastic flow occurred from the center. PT starts in the region with the maximum pressure, i.e., at the center; the pressure gradient and the pressure in the transforming region grow because of the higher yield strength of the product phase which in turn results in the intensification of PT. PT emanates and spreads from the center leading to further pressure growth. Such a positive mechanochemical feedback can lead to a very large pressure growth in the center region because it does not contribute significantly to the total force which is kept constant. Indeed, for B1→B2 PT in KCl, the pressure in the center of the disk has been increased by 50%–70% in Ref. 3 and by a factor of 2 in Ref. 4. For a homogeneous pressure growth in the whole specimen, contribution to the force is much larger, which limits the pressure growth. Also, the pressure growth is related to the differences in elastic properties rather than plastic properties of parent and product phases.

2. Change in turbostratic stacking fault concentration

Change in TSF concentration is presented in Table I. For comparison, under hydrostatic loading up to 9.4 GPa, relative broadening of the peaks and consequently change in s were negligible. This indicates that the disordering of material is *plastic strain induced*. The PT pressure for the initiation of hBN→wBN PT under hydrostatic conditions was found to be 10.4 GPa at $s=0.04$. For comparison, for $s=0.02\pm0.02$, pressure for initiation of hBN→wBN PT was[22,23] $p=8.2\pm0.1$, which is consistent with the tendency that any increase in s increases the PT pressure. Under plastic compression and rotation up to a pressure of 9.6 GPa and total rotation by 160°, s grows from 0.077 to 0.127 at 5.8 GPa and then reduces to 0.107 at 9.6 GPa. Such a growth in s must increase the hBN→wBN phase transformation pressure significantly. During hBN→wBN phase transformation induced by rotation at ~10 GPa by 25°, when $c=0.70$, s suddenly increased to 0.238–0.267. As we will discuss in Sec. V, this can be explained by the TRIP phenomenon only. This is consistent with the small increase in s after an additional rotation of 70° when PT was also arrested due to high s. For comparison, under hydrostatic condition up to 13.4 GPa, degree of disorder was changed during a quite intensive PT ($c\cong0.2-0.4$) from 0.04 to 0.06, which is within the discrepancy of the experiment.[22,23] Note that the center of rotation of the anvil could be shifted with respect to the center of the specimen by 20–40 μm. This means that, before and after rotation, we may measure x-ray pattern at material points with different distances with respect to rotation center, i.e., for particle with different loading history. This explains the reduction in s and c after some rotation stages, along with a general increase in s for most rotation stages. We do not have enough data to separate the effect of compression and rotation on s. The general understanding is that plastic straining and transformation-induced plasticity during compression and shear increase s.

3. PT progress

X-ray diffraction pattern obtained at various pressures during scanning along the diameter are shown in Fig. 5. First traces of wBN, $c=0.05$, were observed after compression up to 9.6 GPa ($\phi=0°$) at $s=0.106-0.127$ based on (110) pattern, Fig. 5(a). A similar evidence is observed in Fig. 5(b)(curve b) when a wBN (100) shoulder appears at 9.6 GPa and 0° rotation. For this strain-induced PT, pressure grows simultaneously with plastic compressive strain. This indicates that PT under even smaller constant pressure can be

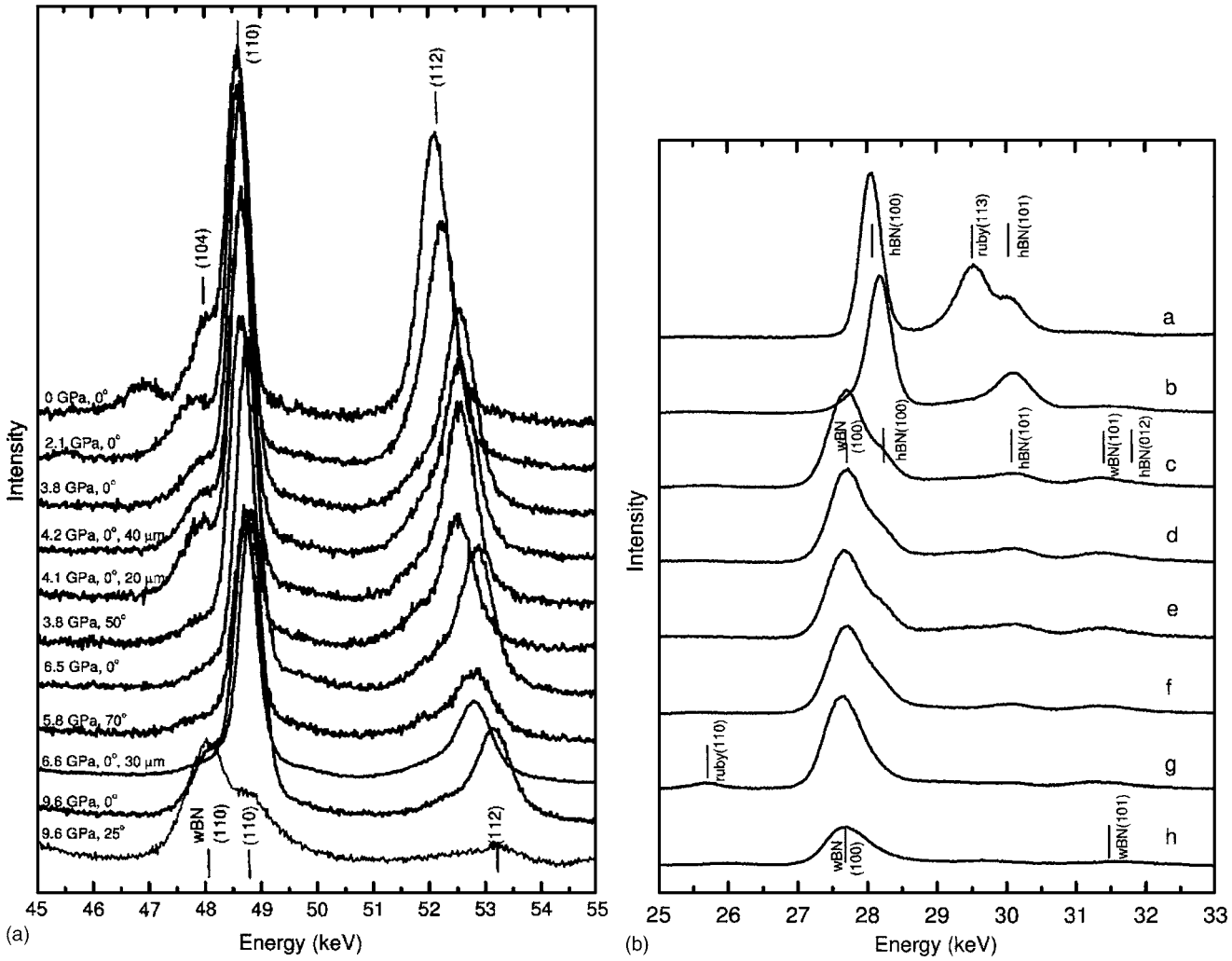

FIG. 5. (a) The progression of broadening of (110) and (112) peaks of boron nitride during compression and shear loading stages; x-ray measurements were performed at the center of the sample, except those marked with micrometer values indicating distance from center. (b) Comparison of x-ray diffraction patterns, (110) peak, of boron nitride during compression and shear loading stages: (a) $p=0$, $\phi=0°$; (b) $p=9.6$ GPa, $\phi=0°$ ($c=0.05$); (c) $\phi=25°$ after conditions described by b at $r=0$ ($c=0.70$); (d)same as c, $r=20$ μm; (e) same as c, $r=40$ μm; (f) $\phi=70°$ after c, $r=0$; and (g) $\phi=205°$, $r=0$.

induced by rotation of the anvil. Volume fraction of wBN reaches 0.70 during a subsequent rotation by 25° (accumulated plastic strain increment Δq is of order of 0.2–0.4) in a pressure range of 9.6–10.3 GPa, along with an increase in TSF concentration to $s=0.238-0.267$. As shown in Table I, further rotation by 70° does not cause the observed PT progress at the center of specimen, most probably because of the high level of s. An additional rotation of $\phi=205°$ completes the PT at a homogenous pressure of $p=10.6$ GPa. Such a PT pressure is surprisingly low for such a high TSF concentration. We remind that in shock experiments at $p=20$ GPa, the volume fraction c of wBN intensively grows with decreasing s from 0 for $s\geqslant 0.1$ to 0.8 for $s=0.03$, wBN was not observed at $s>0.1$, and at $p=30$ GPa, $c<0.6$ for $0.08<s<0.32$.[5] Under hydrostatic pressure, PT was reversible up to $p=10.5$;[8] PT does not complete up to $p=25$ GPa.[23] In Ref. 24, texturized highly ordered hBN started to transform to wBN at $p=10$ GPa under nonhydrostatic conditions; after pressurizing to 12 GPa, wBN was quenchable.

During the rotation of the anvil, we did not observe a significant difference between the PT progress along the radius, which can be explained by TRIP (Sec. V).

After completion of the loading process of the first specimen and upon close examination of the surface of the anvil, particles of sizes up to a few microns were observed to have bonded to the diamond surface. These particles could not be removed by any mechanical instrument, i.e., using sharp and hard instruments. Additionally, scratches with circular patterns were observed, which could not be produced by wBN. Due to small size of the particles, both Raman and synchrotron x-ray techniques yielded inconclusive results on the nature of these particles. Research is continuing to determine the makeup and structure of these particles. We have not ruled out the possibility of a new phase which appear under high local pressure and shear at the contact between wBN particles and diamond.

C. Third sample

A stainless steel gasket with a 60 μm hole radius and an initial thickness of 270 μm was used. X-ray diffraction measurements were performed at the central part of specimen. After compression to 6 GPa, concentration of TSF was measured at 0.124. After rotation of $\phi=360°$, pressure at the

center increased to 7.5 GPa and s grew to 0.218. Further rotation by $\phi=180°$ increased the pressure at the center to 8 GPa. Diffraction peak (112) was completely broadened, i.e., s reached its maximum value $s=1$. Diffraction peak (110) was broadened but still observable. After the last rotation by $\phi=360°$, pressure at the center did not change. hBN peaks (110) and (100) were present, i.e., amorphization did not occur. PT to wBN was not observed. The thickness of the sample after unloading was 44 μm. Despite the extremely large shear and radial flow, the pressure distributions are reasonably homogenous.

V. MODEL AND ANALYSIS: TRIP PHENOMENON AND CASCADE STRUCTURAL CHANGES

As mentioned previously, time is not a relevant parameter for strain-induced PTs; instead, strain-controlled kinetics is considered. Plastic strain history is usually determined in terms of accumulated plastic strain q (Odqvist parameter), $\dot{q}=(\frac{2}{3}\mathbf{d}_p:\mathbf{d}_p)^{0.5}$, where $\mathbf{d}_p$ is the plastic strain rate tensor,[18] tensors are denoted in boldface type, and $\mathbf{A}:\mathbf{B}=A_{ij}B_{ji}$ is the contraction of tensors over two indices. Based on our experiments, we are unable to determine the distribution of q. However, the analytical solution for the plastic problem on deformation under rotation under fixed force shows[8,19] that q is scaled with the rotation angle ϕ of the anvil, and accordingly, we will use ϕ as an independent strainlike parameter.

A. Strain- and TRIP-induced turbostratic stacking fault generation

For TSF generation, the following evolution equation is accepted:

$$\dot{s}=m\dot{\phi}+n\dot{c}, \tag{3}$$

where ϕ is in radians. Since pressure itself does not change s, $s=$const when ϕ and c are fixed. Assuming constant parameters m and n, we obtain

$$s=s_0+m(\phi-\phi_0)+n(c-c_0). \tag{4}$$

Our five experiments without PT (second sample, change in s from $s=0.082$ to 0.094 due to rotation by $\phi=50°$ at 4 GPa; change in s from $s=0.098$ to 0.103 due to rotation by $\phi=20°$ and from $s=0.103$ to 0.127 due to rotation by $\phi=70°$ at 6 GPa; change in s from $s=0.266$ to 0.278 due to rotation by $\phi=70°$ at 10 GPa, when $c=0.7$ did not change; third sample, and change in s from $s=0.124$ to 0.218 due to rotation by $\phi=360°$ in the pressure range of 6–7.5 GPa) are well described by $m=0.017$. Thus, m is independent of ϕ, p, and c. The parameter $n=0.235$ was determined from the loading step 10 in Table I. For large $\phi>360°$ (third sample, second rotation by $\phi=180°$) the obtained $m=0.25$ is much higher. The reason for such an increase is to be determined.

It follows from the model (see below) that, during the PT, the major part of disorder is due to a change in volume faction c of wBN rather than due to shear ϕ. The following question arises: Why does a growth in c induce disorder? One may assume that hBN→wBN PT occurs predominantly in the well-ordered regions of the hBN crystal lattice, which has to increase s even without further strain-induced disordering. However, we obtained experimentally that the change in s during the PT under hydrostatic condition is negligible. The only reasonable explanation is based on TRIP phenomenon that is well studied for uniaxial loading of steels and geological materials under normal pressure,[11] but not in any known high pressure experiments in diamond anvil cell. Volumetric transformation strain ε_0 during any PT creates large internal stresses which in combination with external nonhydrostatic stresses lead to TRIP (Greenwood-Johnson effect). As it follows from our analytical solution for PT or chemical reaction for shear under pressure,[8,12] transformation-induced plastic shear during the complete PT, γ, is determined by the equation $\gamma=\varepsilon_0[\tau/\tau_y/\sqrt{1-(\tau/\tau_y)^2}]$, where τ is the shear stress. Shear strain rate is proportional to $\dot{c}$; thus $\dot{\gamma}=\varepsilon_0[\tau/\tau_y/\sqrt{1-(\tau/\tau_y)^2}]\dot{c}$ (we assume that τ does not vary during the PT). When shear stress approaches the yield stress in shear, TRIP shear tends to infinity. For hBN→wBN phase transformation, transformation-induced plasticity has to be much stronger than in steels since for steels $\varepsilon_0=0.02-0.05$ and for hBN→wBN PT, $\varepsilon_0=0.53$. Usually, TRIP is determined experimentally under external stresses below the yield stress (stress-induced PT); thus traditional plasticity is absent and TRIP can be measured. In strain-induced experiments, plastic flow takes place even without PT; thus it is difficult to prove the existence of TRIP directly. However, existence of part of $\dot{s}$ proportional to $\dot{c}$ is the signature of the existence of part of plastic shear proportional to $\dot{c}$, i.e., *existence of TRIP*.

Note that rotation angle of an anvil, ϕ, is a convenient measurable geometric characteristic of plastic deformation but is not a physically meaningful one, because it does not reflect the state of the material. Also, rotation angle of the sample is smaller than rotation angle of the anvil ϕ because of relative sliding; ϕ does not characterize the compression stage. In metal plasticity, dislocation density and/or grain size are usually used. Since disorder is strain-induced, increment Δs is proportional to the total plastic strain increment independent of whether it is caused by external stress or by TRIP. Thus, for hexagonal systems, a change in s can be considered as a natural physical measure of plastic strain, evolution of which can be determined *in situ*. Changes in s can characterize plastic strain under arbitrary complex loadings, in particular, during the compression stage. Then Eq. (2) allows us to separate the conventional plasticity, $\Delta s_p=m\Delta\phi$, and TRIP, $\Delta s_t=n\Delta c$. In our experiments, rotation by $\Delta\phi=0.436$ at 9.6 GPa leads to $\Delta s=0.160$ and $\Delta c=0.65$. Thus $\Delta s_p=0.007$ and $\Delta s_t=0.153$, i.e., TRIP exceeds the conventional plasticity by a factor of 20. This makes our proof independent of any possible experimental errors and is consistent with prediction of the equation for γ when shear stress approaches the yield stress. This also solves the paradox of why we did not find a difference in c along the radius of the sample, despite the fact that shear strain for torsion is proportional to the radius: TRIP is proportional to shear stress rather than strain which is practically independent of radius for plastic torsion. TRIP is the same as a usual plasticity but is caused by internal plus external stresses rather than by external stresses only. That is why TRIP, in the same way as usual plasticity, generates the TSF (the dominating

part) and new nucleating defects. Thus, we arrive at the cascade mechanism of structural changes during rotation of an anvil (Fig. 1).

B. Phase transformation criterion

The transformation deformation gradient $\mathbf{F}_t$ transforms a stress-free crystal lattice of hBN into a stress-free crystal lattice of wBN. In the simplest case, when the temperature θ is fixed and homogeneous in a transforming volume V_n, with a mass m_n, the net thermodynamic driving force for PT, F, in the volume V_n bounded by surface Σ is as follows:[9,10,19,26]

$$F := (X-K)m_n = \int_{m_n}\int_{\mathbf{I}}^{\mathbf{F}_{t2}} \frac{1}{\rho}\mathbf{T}:(d\mathbf{F}_t\cdot\mathbf{F}_t^{-1})dm_n - \int_{m_n}\int_{\mathbf{E}_1}^{\mathbf{E}_2}\frac{1}{2\rho}\varepsilon_e:d\mathbf{E}:\varepsilon_e dm_n - (\Delta\psi(\theta)+K)m_n - \Gamma\Sigma. \tag{5}$$

Here, X is the driving force for phase transformation, which represents the dissipation increment due to PT only (i.e., excluding all other types of dissipation, e.g., plastic dissipation) during the entire transformation process averaged over the transforming region, K is the dissipation due to PT related mostly to interface friction, $\mathbf{T}$ is the true (Cauchy) stress tensor, ρ is the variable mass density during the phase transformation, $\Delta\psi$ is the jump in the thermal part of the free energy, $\mathbf{E}$ is the tensor of elastic moduli, ε_e is the elastic strain, Γ is the surface energy per unit area, the indices 1 and 2 denote the values before and after PT, and ":=" means equal per definition. The first term on the right hand side of Eq. (5) represents the transformation work which takes into account the whole history of stress tensor variation. For elastic materials, the expression for X coincides with a change in the Gibbs free energy of the whole system per unit mass,[10] i.e., as in a standard approach.

Let us make the following simplifications. We decompose the stress tensor $\mathbf{T}$ into the sum of the macroscopic part $\boldsymbol{T}_m$, which is homogeneous in a representative volume $V \gg V_n$, and the microscopic contribution $\tilde{\boldsymbol{T}}$, which fluctuates inside volumes V and V_n. As $V \gg V_n$, the variation of the macroscopic stress $\boldsymbol{T}_m$ is negligible during a small phase transformation increment. Maximum macroscopic shear stress τ_m is limited by the macroscopic yield stress, which is negligible in comparison with the pressure. Then, the thermodynamic PT criterion, $F=0$,[9,10,19,26] can be resolved with respect to the macroscopic pressure $p=\frac{1}{3}\mathbf{I}:\mathbf{T}$:

$$p = \left(-\int_{V_n}\int_{\mathbf{I}}^{\mathbf{F}_{t2}}\frac{1}{\rho}\tilde{\mathbf{T}}:(d\mathbf{F}_t\cdot\mathbf{F}_t^{-1})dm_n + \int_{m_n}\int_{\mathbf{E}_1}^{\mathbf{E}_2}\frac{1}{2\rho}\varepsilon_e:d\mathbf{E}:\varepsilon_e dm_n + (\Delta\psi(\theta)+K) - \Gamma\Sigma\right)\frac{\rho_1}{m_n\varepsilon_0}, \tag{6}$$

where $\varepsilon_0=\det\mathbf{F}_t$ is the volumetric transformation strain. To evaluate the integral in Eq. (6), we have to know the specific mechanism of nucleation and stress concentration at the nucleating defects and to solve the corresponding boundary-value problem numerically. This is a separate complex problem with many unknown parameters, which was treated in the literature under various assumptions.[8–12,19,26] Here we will suggest the simplest approximation of Eq. (6) in terms of the measurable macroscopic parameter which will be fitted to experimental data. Because of different mechanisms of pressure- and strain-induced PTs, approximations will be different as well.

C. Pressure-induced phase transformation

We consider thermally activated nucleation of critical nuclei at defects and their growth until they are getting arrested by a strong obstacle (grain or twin boundaries, turbostratic stacking fault, or other wBN region). Thus, time is not a parameter and Eq. (6) may be approximated in the following form:

$$p = p_0 + A(c-0.05) + Bs, \tag{7}$$

where A, p_0, and B are constants and volume fraction $c=0.05$ is accepted as the smallest concentration that can be detected experimentally. There are various defects with various magnitudes of stress concentration, which determine the distribution of their potency for nucleation. First, nucleation occurs at strongest defects, and after growth is arrested, PT stops as well. It is necessary to increase the pressure to activate the nucleation site of lower potency and produce the next increment Δc, and so on. This process is mimicked by approximation of the integral by the term $A(c-0.05)$. The effect of concentration of TSF on PT pressure is quantitatively explained in Ref. 5 by the condition that the width of the critical nucleus is limited by the distance between two nearest TSFs. We may add that even if the width of critical nucleus is smaller than this distance, its growth may be arrested by the nearest TSF or TSF will increase the resistance to interface motion. Thus the larger s is, the smaller the increment of c that can be produced by the same nucleating defects, which is mimicked by the term Bs.

As it was obtained experimentally, under hydrostatic loading, changes in s are negligible with and without PT; therefore, s can be considered as an initial or a current value. The following parameters were obtained using data from Ref. 5:

$$p_0 = 3.333\ \text{GPa}, \quad A = 17.54, \quad B = 175.44 \quad \text{for } 0 < s < 0.1, \tag{8}$$

$$p_0 = 20.26\ \text{GPa}, \quad A = 17.54, \quad B = 6.14 \quad \text{for } s > 0.1. \tag{9}$$

It is clear that the effect of c on the phase transformation criterion is the same for any s; however, the effect of s is much smaller for $s>0.1$. Relationships between c and s for $p=20$ and 30 GPa based on Eqs. (8) and (9) perfectly describe experimental data in Ref. 5. Equation (8) also perfectly describes our experiment for initiation of PT [$c=0.05$, $p=10.4$, and $s=0.04$ for both Eq. (8) and experiment] and correctly describes data from Ref. 23 [$c=0.05$, $p=8.2$, and

$s=0.028$ for Eq. (8) and in experiment $s=0.02\pm0.02$]. For $s=0.028$ and $c=1$, one obtains $p=24.9$ GPa, which is in good agreement with data in Ref. 22 that PT was not completed at 25 GPa.

D. Strain-induced phase transformation

It is well known[19,25] that strain-induced nucleation occurs at new defects generated during plastic flow. Some of these defects may produce much higher stress concentration than preexisting defects. Stress concentration near the defects significantly increases the driving force for the phase transformation and can cause PT at significantly lower external pressure. It leads to barrierless nucleation, which does not require thermal fluctuations, and explains the strain-controlled rather than time-controlled kinetics.[19,26] Indeed, the prescribed strain increment generates defects (dislocation pileups or tilt boundary at various shear-band intersections) with barrierless, i.e., very fast, nucleation and growth of the new phase up to the size where stress concentration is reduced and cannot drive the interface further. As straining stops, no new defects and nuclei appear, and the growth of the existing nuclei is thermodynamically impossible. All of these results were conceptually incorporated in our microscale model.[19,27]

Our model here represents a generalization of the model presented in Ref. 19 and 27 for the case which takes into account TSF and TRIP. For strain-induced nucleation, one needs to add the transformation work of local stresses due to defects generated during the plastic flow to the equation for the driving force [Eq. (6)]. We approximate this extra transformation work divided by volumetric transformation strain by additional terms in phase transformation criterion (7):

$$p+\Delta p\left(1-\frac{\bar{a}}{(1-c)}\left(\frac{dc}{dq_1}\right)\right)+A(1-\nu)c = p_0+A(c-0.05)+Bs. \tag{10}$$

Here q_1 is the accumulated plastic strain in the parent phase 1; Δp, $\bar{a}$, and ν are parameters; the factor $(1-c)$ takes into account that PT occurs in the hBN phase only. The first additional term in Eq. (10) was introduced in our recent papers[19,27] based on finite element analysis of nucleation at shear-band intersection[28] and nucleation at dislocation pileup.[19,26] Qualitatively, this contribution has to be similar for any mechanism of nucleation at strain-induced defects, because stress decreases sharply away from a defect. Thus, for small prescribed strain increment Δq_1, the larger is the nucleus and consequently Δc, the smaller is the stress averaged over the nucleus and driving force for the phase transformation. The term $A(1-\nu)c$ characterizes the generation of new nucleating defects due to TRIP caused by the interaction of external nonhydrostatic stress fields with internal stresses due to large transformation volumetric strain.[11,12] To define the Odqvist parameter for each phase q_i, we assume[19,27] $q=(1-c)q_1+cq_2$ and $q_1/q_2=(\sigma_{y1}/\sigma_{y2})^w$, from which

$$q_1=q\frac{\sigma_{y2}^w}{c\sigma_{y1}^w+(1-c)\sigma_{y2}^w},\quad q_2=q\frac{\sigma_{y1}^w}{c\sigma_{y1}^w+(1-c)\sigma_{y2}^w}. \tag{11}$$

Here q is the Odqvist parameter of a two-phase mixture, σ_{yi} is the yield stress of ith phase, and w is a parameter. Since the yield stress of wBN $\sigma_{y2}\gg\sigma_{y1}$ for hBN, one obtains from Eq. (11) $q_1=q/(1-c)$ and $([\bar{a}/(1-c)](dc/dq_1))=\bar{a}(dc/dq)=a(dc/d\phi)$, where proportionality between q and ϕ is taken into account (a is a parameter). Thus two contributions that plastic strain is localized in the weak hBN $[q_1=q/(1-c)]$ and that phase transformation occurs in hBN phase only eliminate each other. Solving Eq. (10) for $dc/d\phi$ and taking into account Eqs. (4) and (11), one obtains a thermodynamically consistent strain-controlled kinetic equation

$$dc/d\phi=Y\geqslant 0, \tag{12}$$

with $Y:=J-bc-N\phi$, $b:=(A\nu+Bn)/(a\Delta p)$, $J:=(p+\Delta p-p_0+0.05A-B(s_0+m\phi_0+nc_0))/(a\Delta p)$, and $N:=Bm/(a\Delta p)$.

If $Y<0$, then $dc/d\phi=0$. Solution to the evolution equation (12) satisfying the initial condition $c(\phi_0)=c_0$ is

$$c=[bJ+N-bN\phi+e^{b(-\phi+\phi_0)}(-N+b(bc_0-J+N\phi_0))]/b^2. \tag{13}$$

This solution is valid for ϕ up to which all conditions

$$Y\geqslant 0,\quad c\leqslant 1,\quad s=s_0+m(\phi-\phi_0)+n(c-c_0)\leqslant 1 \tag{14}$$

are satisfied. If c reached 1, it does not change anymore. If pressure (and consequently J) is lower than some critical value, the condition $Y=0$ is fulfilled for some value of ϕ_m and $c=c_{\max}<1$, where $c_{\max}$ is the maximum value of c. Further rotation does not change c anymore, unless pressure p increases and $Y>0$ again. Also, rotation that does not cause PT increases s, which in turn increases the level of pressure p required for reinitiation of PT.

There are three material parameters to be determined, namely, a, Δp, and ν. Analysis shows that the parameter a weakly affects $c_{\max}$. Thus using two values of $c_{\max}$ corresponding to two different pressures, one can determine Δp and ν. The parameter a is determined from the experimental value of ϕ_m. We do not have enough experimental points to determine these parameters unambiguously: however, a possible reasonable choice is $\Delta p=14.9$ GPa, $\nu=0.07$, and $a=0.35$. A small value of ν means [according to Eq. (10)] that defect generation due to TRIP almost *reproduces* preexisting defects already utilized for wBN nucleation. Using these data, $s_0=0.107$ (see Table I, loading step 9), and $c_0=0$, one obtains from Eq. (13) that a detectable amount of wBN, $c=0.05$, can be obtained at a pressure of 6.3 GPa, while complete strain-induced PT can occur at $p=9.3$ GPa. In comparison, under hydrostatic loading [Eq. (7)] with a fixed $s=0.107$, a detectable amount of wBN, $c=0.05$, can be obtained at a pressure of 20.9 GPa, while a complete strain-induced PT can occur at $p=37.6$ GPa. These numbers demonstrate a very strong reduction of pressure for hBN to wBN phase transformation due to plastic shear: by a factor of 3 for initiation of PT and by a factor of 4 for completing.

In Fig. 6, the relationship between the volume fraction c of wBN and rotation angle ϕ for various pressures is shown for $s_0=0.107$. Substituting Eq. (13) in Eq. (4) for s, one

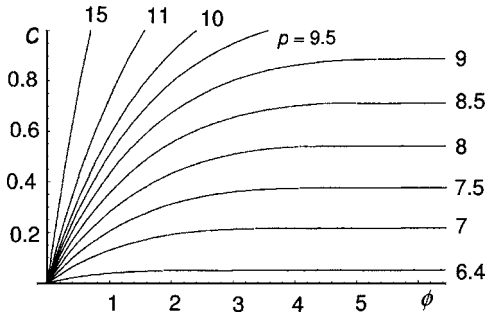

FIG. 6. Calculated relationship between the volume fraction of wBN c and rotation angle ϕ for various pressures and $s_0=0.107$ (shown in GPa near the curves).

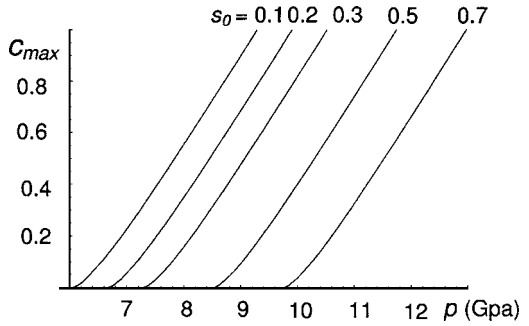

FIG. 8. Calculated relationship between the pressure and maximum volume fraction $c_{\max}$ of wBN for various initial concentrations of turbostratic stacking fault s_0 (shown near the curves).

obtains the corresponding relationship between s and ϕ for various pressures (Fig. 7). Dots which end curves for $p>9.5$ correspond to $c=1$ and disappearance of hBN. For $\phi>\phi_m$, corresponding to constant c, one obtains $s=s_0+m(\phi-\phi_m)+n(c_{\max}-c_0)$, i.e., set of parallel lines for various pressures; dashed line corresponds to $c_{\max}=1$. The strong deviation (especially at high pressure) of $s(\phi)$ curves in Fig. 7 from these parallel lines during intense PT shows that the major contribution of disorder is due to transformation-induced plasticity; TRIP exceeds significantly conventional plasticity. For all cases, s does not exceed 0.4, i.e., restriction $s<1$ is not essential.

Condition $Y=0$ determines the angle ϕ_m corresponding to maximum volume fraction c:

$$\phi_m=\phi_0+\ln[(N+b(-bc_0+J-\phi_0N))/N]/b. \tag{15}$$

Substituting Eq. (15) in Eq. (13), one obtains the maximum value of wBN volume fraction

$$c_{\max}=(b(J-\phi_0N)-N\ln[(N+b(-bc_0+J-\phi_0N))/N])/b^2. \tag{16}$$

Starting with the pressure at which $c_{\max}$ reaches 1, the angle ϕ_m has to be determined from the condition $c_{\max}=1$ in Eq. (13). The plots for $c_{\max}$ and ϕ_m versus pressure p for various s_0 are shown in Figs. 8 and 9. On the decreasing branch of the curves $\phi_m(p)$, the condition $c_{\max}=1$ is met. For any s, the maximum rotation angle to complete PT does not exceed 5.5 rad (315°); thus the traditional wisdom "the larger rotation, the better" does not work because of disordering. At $p\sim10$ GPa, PT is completed before $\phi=295°$, as in experiment 2. The difference between experiment and model in s is related solely to a difference in c; for proper c, coincidence is very good. Our model gives also reasonable description of the third experiment, where wBN was not observed. For $\phi=360°$, $s_0=0.124$, and $p=6.2$ GPa, the model does not predict any wBN and predicts a change in s to 0.231 (0.218 in experiment). For the second rotation by 180°, one needs to use $m=0.25$. The model predicts that $c_{\max}=0.05$ can be obtained at $p=7.9$ GPa and rotation by 32°, which is in reasonable agreement with experiments in which phase transformation was not observed at $p\sim8$ GPa. During second rotation by 180°, s reaches 1 both in experiment and model. After this, PT cannot be detected in both experiment and model. If condition $s=1$ is met, it has to be substituted in Eq. (10) instead of Eq. (4) which results in the following evolution equation:

$$\frac{dc}{d\phi}=J_1-b_1c\geqslant 0,$$

$$J_1:=\frac{(p+\Delta p-p_0+0.05A+B)}{a\Delta p},\quad b_1:=\frac{A\nu}{a\Delta p} \tag{17}$$

and its solution

$$c=\frac{e^{b_1(-\phi+\phi_0)}(b_1c_0-J_1)+J_1}{b_1}. \tag{18}$$

Maximum volume fraction $c_{\max}=J_1/b_1$ is reached at $\phi\to\infty$ if $J_1/b_1\leqslant 1$ or $c_{\max}=1$ otherwise. Thus, for completely disordered hBN and $J_1/b_1\leqslant 1$, larger ϕ is better. Note that the

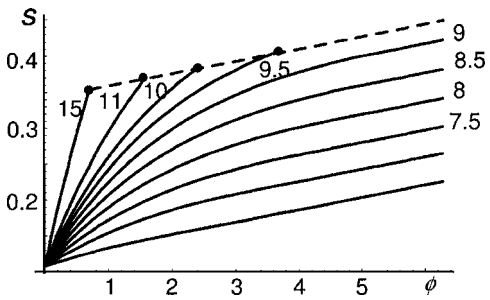

FIG. 7. Calculated relationship between the concentration of turbostratic stacking fault s and rotation angle ϕ for various pressures (shown in gigapascals near the curves).

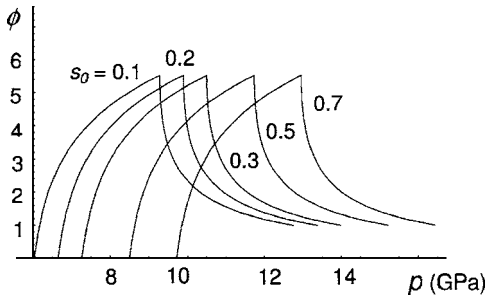

FIG. 9. Calculated relationship between the pressure and rotation angle ϕ necessary to reach maximum volume fraction $c_{\max}$ of wBN for various initial concentrations of turbostratic stacking fault s_0 (shown near the curves).

results for $s=1$ have to be considered with caution because such high value of s is far from that studied experimentally. In particular, hBN→cBN PT or amorphization may occur instead.

VI. CONCLUDING REMARKS

In this work, strain-induced disorder and martensitic hBN→wBN PT were studied locally, under compression and shear, in a rotational diamond anvil cell using *in situ* x-ray diffraction with synchrotron radiation. We succeeded in obtaining an almost homogeneous pressure in hBN and the resulting wBN along the radius of a sample. This was based on the theoretical analyses of plastic flow and friction which resulted in the conclusion that plastic flow to the center of a sample has to occur, at least during the compression stage. Homogeneous pressure in a sample was obtained using a gasket with theoretically estimated gasket-hole dimensions. We observed for the first time the "homogeneous pressure self-multiplication effect." Namely, despite the significant volume decrease by a factor of 1.53, pressure grows almost homogeneously in the transforming region. The disorder of hBN did not change under hydrostatic loading up to 9.43 GPa. However, disorder grows from an initial value of $s=0.08$ to $s=0.1-0.13$ in a pressure range of 6.3–9.6 GPa under shear (before beginning of PT). This increase neutralizes the transition pressure reduction caused by shear. However, a complete irreversible strain-induced transformation hBN→wBN was observed in the whole specimen at a surprisingly small (for such a disorder) pressure of 9.6–10.6 GPa and rotation of $\phi=325°$. During strain-induced PT, disorder s increased drastically to 0.238–0.278, while under pressure-induced PT, the change in disorder was negligible. Thus, the disorder is strain and PT induced. Analysis of changes in s led us to the conclusion that s can be used as a natural physical measure of plastic straining under arbitrary complex loading, evolution of which can be determined *in situ*. It also allowed us to prove the existence of the TRIP phenomenon and to separate TRIP from usual plasticity. Since TRIP exceeds the conventional plasticity by a factor of 20, actual plasticity involved in the PT process is much larger than the prescribed one (this was neglected in literature). TRIP allows us to complete PT at much lower pressure. It also makes all hBN-wBN interfaces semicoherent, which arrests the reverse PT after complete unloading and allows us to obtain complete irreversible phase transformation. TRIP also solves the paradox that we did not find a difference in c along the radius of the sample, despite the fact that shear strain for torsion is proportional to the radius: TRIP is proportional to shear stress rather than strain which is practically independent of radius for plastic torsion.

Formation of small strong particles of yet unidentified structure which scratched the diamond anvil and strongly bonded to the diamond surface was also observed. Coupled strain-controlled kinetic equations for concentration s and volume fraction c of wBN were derived and their analytical solutions were analyzed. We obtained the following results. (a) For the same initial disorder, plastic shear indeed reduced the PT pressure significantly (by a factor of 3 for initiation and 4 for completing) in comparison with hydrostatic loading. (b) For relatively small constant p, strain-induced PT is arrested at some value c_{max} due to increase in s. (c) Rotation angle to obtain the maximum value c_{max} does not exceed 5.5 rad (315°); thus the traditional wisdom "the larger the rotation angle, the better" does not work because of disordering. (d) For $s_0=0.11$, pressures for initiation and completing the PT are 6.3 and 9.3, respectively. (e) Function $c_{max}(p)$ was also obtained for various initial disorders. The results provide basic information on physics of interaction between plastic straining, disordering, and PTs, including kinetics and irreversibility aspects. The cascade structural changes were revealed (Fig. 1).

We believe that similar results are valid for PT in all hexagonal and rhombohedral crystals, sensitive to disorder and with appreciable ε_0. As an example, we mention PT from low density hexagonal and rhombohedral modifications of BN and graphite to high density superhard cubic and hexagonal BN and diamond. Strong TRIP is expected to be found for strain-induced phase transformation in any material with large ε_0 (according to theories[8,11,12]); however, to prove its existence and to quantify it, some strain measures (similar for s in hexagonal and rhombohedral crystals) have to be found. Also, strong transformation-induced plasticity and cascade mechanisms are expected to be found in shear bands, which has to be taken into account, e.g., for analyses of the earthquakes[29] and chemical reactions.[12]

This study also shows directions in which further research has to proceed. To identify the displacement and strain fields, one needs to determine the relative position of rotation and specimen centers, as well as to measure displacement of ruby particles.[21] One needs to individualize a number of ruby particles, used for pressure and displacement measurements, and to measure diffraction patterns in their vicinity. Then we would be able to determine, locally, how s and c vary in material particles (rather than spatial locations) under a prescribed pressure and plastic strain history. To find such a dependence, one needs to produce large rotations under smaller pressure in the range of 4–8 GPa; at higher pressure, the rotation increment has to be much smaller (2°–4°). To reduce the PT pressure, increase c, and to determine the minimal pressure below which PT is impossible under any strain, we need to start with highly ordered precursor material and to reduce (avoid) plastic straining during the compression stage. Once a suitable pressure level is reached, a large level of rotation can then be introduced to produce PT. If PT was not obtained at the chosen pressure and large rotation, this specimen should not be used at higher pressure; it is spoiled. To decrease plastic strain, one needs to start with a smaller gasket thickness, use highly textured material, or use hydrostatic media which solidifies just below the pressure of interest. For $s\cong 0.1$, our model predicts appearance of first detectable amount of wBN at 6.3 GPa. We expect smaller phase transformation pressure for smaller initial s; however, we do not have experimental data for $s<0.1$ to make quantitative modeling.

At the same time, an increase in s to high values can promote diffusive PT. Indeed, at $p=11$ GPa and $s>0.3$, reconstructive hBN→cBN phase transformation (rather than

martensitic hBN→wBN phase transformation) starts at temperatures above 800 K; above $s=0.4$, the temperature for hBN→cBN PT even decreases slightly with increasing s and is about 800 K at $s=1$.[7] The hBN→cBN PT has never been observed at room temperature. If in our first experiment cBN was observed, it may have occurred in the region of highly disordered residual hBN. We would not exclude even complete amorphization of residual hBN because of extremely large plastic strain and pressure during its deformation between strong wBN particles. It is known, in particular, that amorphization of hBN occurs during ball milling which represents large dynamic plastic straining under local pressure of 4–8 GPa.[30] Amorphization also reduces the PT temperature for the reconstructive PT hBN→cBN.[30]

ACKNOWLEDGMENTS

Support from Texas Tech Excellence Fund is gratefully acknowledged. Two of the authors (V.I.I. and M.H.) acknowledge partial support from the National Science Foundation (CMS-0555909 and ECS 0323640, respectively).

[1] P. W. Bridgman, Phys. Rev. **48**, 825 (1935); Proc. Am. Acad. Arts Sci. **71**, 387 (1937); J. Chem. Phys. **15**, 311 (1947).
[2] L. F. Vereschagin, E. V. Zubova, K. P. Burdina, and G. L. Aparnikov, Dokl. Akad. Nauk SSSR **196**, 81 (1971).
[3] V. D. Blank, Yu. Ya. Boguslavski, M. I. Eremetz, E. S. Izkevich, Yu. S. Konyaev, A. M. Shirokov, and E. I. Estrin, JETP **87**, 922 (1984); M. M. Aleksandrova, V. D. Blank, A. E. Golobokov, Yu. S. Konyaev, and E. I. Estrin, Solid State Phys. **29**, 2573 (1987); M. M. Alexandrova, V. D. Blank, and S. G. Buga, *ibid.* **35**, 1308 (1993); N. R. Serebryanaya, V. D. Blank, and V. A. Ivdenko, Phys. Lett. A **197**, 63 (1995); V. D. Blank, M. Popov, S. G. Buga *et al.*, *ibid.* **188**, 281 (1994).
[4] N. V. Novikov, S. Polotnyak, L. Shvedov, and V. I. Levitas, J. Superhard Mater. **3**, 39 (1999).
[5] V. F. Britun and A. V. Kurdyumov, High Press. Res. **17**, 101 (2000).
[6] A. V. Kurdyumov, Sov. Phys. Crystallogr. **20**, 969 (1975).
[7] A. V. Kurdyumov, V. G. Malogolovetz, N. V. Novikov, A. N. Pilyankevich, and L. A. Shulman, *Polymorphic Modifications of Carbon and Boron Nitride* (Metallurgy, Moscow, 1994).
[8] V. I. Levitas, J. Mech. Phys. Solids **45**, 923 (1997); **45**, 1203 (1997).
[9] V. I. Levitas and L. Shvedov, Phys. Rev. B **65**, 104109 (2002).
[10] V. I. Levitas, Int. J. Solids Struct. **35**, 889 (1998); Int. J. Plast. **16**, 805 (2000); **16**, 851 (2000).
[11] G. W. Greenwood and R. H. Johnson, Proc. R. Soc. London, Ser. A **283**, 403 (1965); G. B. Olson, in *Deformation, Processing and Structure*, edited by G. Krauss (ASM International, Warrendale, PA, 1984), pp. 391–424; F. D. Fischer, Q.-P. Sun, and K. Tanaka, Appl. Mech. Rev. **49**, 317 (1996); V. F. Zackay, E. R. Parker, D. Fahr, and R. Busch, Trans. Am. Soc. Met. **7**, 252 (1967); C. Schmidt, D. Bruhn, and R. Wirth, Earth Planet. Sci. Lett. **205**, 273 (2003); D. C. Dunand, C. Schuh, and D. L. Goldsby, Phys. Rev. Lett. **86**, 668 (2001).
[12] V. I. Levitas, V. F. Nesterenko, and M. A. Meyers, Acta Mater. **46**, 5929 (1998); **46**, 5947 (1998).
[13] V. I. Levitas, J. Hashemi, and Y. Ma, Europhys. Lett. **68**, 550 (2004); V. I. Levitas, Y. Z. Ma, and J. Hashemi, Appl. Phys. Lett. **86**, 071912 (2005).
[14] J. Z. Hu, H. K. Mao, J. F. Shu, and R. J. Hemley, in *High-Pressure Science and Technology-1993*, edited by S. C. Schmit, J. W. Shaner, G. A. Samara, and M. Ross (AIP, New York, 1994), p. 441.
[15] H. K. Mao and P. M. Bell, Science **191**, 851 (1976).
[16] I. Petrusha (private communications).
[17] R. Jenkins and R. L. Snyder, *Introduction to X-ray Powder Diffractometry* (Wiley, New York, 1996), pp. 16–19.
[18] V. I. Levitas, *Large Deformation of Materials with Complex Rheological Properties at Normal and High Pressure* (Nova Science, New York, 1996); E. G. Thomsen, Ch. T. Yang, and Sh. Kobayashi, *Mechanics of Plastic Deformation in Metal Processing* (The Macmillan Company, New York, 1965).
[19] V. I. Levitas, Phys. Rev. B **70**, 184118 (2004); V. I. Levitas, in *High Pressure Surface Science and Engineering*, edited by Y. Gogotsi and V. Domnich (Institute of Physics, Bristol, 2004), pp. 159–292.
[20] V. D. Blank, N. R. Serebryanaya, A. A. Vorontsov, and A. Yu. Zerr, High Pressure Physics and Engineering **3**, 36 (1993).
[21] V. D. Blank and S. G. Buga, Instrum. Exp. Tech. **36**, 149 (1993).
[22] V. L. Solozhenko, G. Will, and F. Elf, *HASYLAB Jahresbericht 1995* (HASYLAB, Hamburg, 1996), Pt. 2, p. 507.
[23] V. L. Solozhenko and F. Elf, J. Superhard Mater. **3**, 67 (1998).
[24] T. Taniguchi, T. Sato, W. Utsumi, T. Kikegawa, and O. Shimomura, Appl. Phys. Lett. **70**, 2392 (1997).
[25] G. B. Olson and M. Cohen, J. Less-Common Met. **28**, 107 (1972).
[26] V. I. Levitas, Phys. Lett. A **327**, 180 (2004).
[27] V. I. Levitas, Europhys. Lett. **66**, 687 (2004).
[28] V. I. Levitas, A. V. Idesman, and G. B. Olson, Acta Mater. **47**, 219 (1999).
[29] H. Green and P. Burnley, Nature (London) **341**, 773 (1989).
[30] Y. Huang and Y. T. Zhu, Chem. Mater. **14**, 1873 (2002).